

Carbon dioxide adsorption in chemically activated carbon from sewage sludge

Juan Manuel de Andrés,* Luis Orjales, Adolfo Narros, María del Mar de la Fuente, and María Encarnación Rodríguez

Department of Chemical and Environmental Engineering, Technical University of Madrid (UPM), Madrid, Spain

*Please address correspondence to: Juan Manuel de Andrés, Department of Chemical and Environmental Engineering, Technical University of Madrid (UPM), c/ José Gutiérrez Abascal 2, 28006 Madrid, Spain; e-mail: jdeandres@etsii.upm.es

In this work, sewage sludge was used as precursor in the production of activated carbon by means of chemical activation with KOH and NaOH. The sludge-based activated carbons were investigated for their gaseous adsorption characteristics using CO₂ as adsorbate. Although both chemicals were effective in the development of the adsorption capacity, the best results were obtained with solid NaOH (SBA_{TI6}). Adsorption results were modeled according to the Langmuir and Freundlich models, with resulting CO₂ adsorption capacities about 56 mg/g. The SBA_{TI6} was characterized for its surface and pore characteristics using continuous volumetric nitrogen gas adsorption and mercury porosimetry. The results informed about the mesoporous character of the SBA_{TI6} (average pore diameter of 56.5 Å). The Brunauer-Emmett-Teller (BET) surface area of the SBA_{TI6} was low (179 m²/g) in comparison with a commercial activated carbon (Airpel 10; 1020 m²/g) and was mainly composed of mesopores and macropores. On the other hand, the SBA_{TI6} adsorption capacity was higher than that of Airpel 10, which can be explained by the formation of basic surface sites in the SBA_{TI6} where CO₂ experienced chemisorption. According to these results, it can be concluded that the use of sewage-sludge-based activated carbons is a promising option for the capture of CO₂.

Implications: Adsorption methods are one of the current ways to reduce CO₂ emissions. Taking this into account, sewage-sludge-based activated carbons were produced to study their CO₂ adsorption capacity. Specifically, chemical activation with KOH and NaOH of previously pyrolyzed sewage sludge was carried out. The results obtained show that even with a low BET surface area, the adsorption capacity of these materials was comparable to that of a commercial activated carbon. As a consequence, the use of sewage-sludge-based activated carbons is a promising option for the capture of CO₂ and an interesting application for this waste.

Introduction

Recent scientific evidences show that there is a clear correlation between global warming and the concentration of greenhouse gases (GHGs) in the atmosphere (Intergovernmental Panel on Climate Change [IPCC], 2007). According to current climate change mitigation policies and related sustainable development practices, global GHG emissions will continue to grow over the next few decades (IPCC, 2007; Zecca and Chiari, 2010). Thus, it is necessary to find out different ways to reduce the GHG emissions (especially of CO₂) to try to diminish the negative impact of these gases over the climate in the future years.

Some of the current ways to reduce CO₂ emissions are the efficient conversion of fossil fuels (Adams and Barton, 2011; Lanzi et al., 2011), the use of low-carbon fossil fuels (Beér, 2007; Polyzakis et al., 2008), carbon capture and storage (Adams and Barton 2010; Peng et al., 2012), and the use of renewable energy (Gross et al., 2003; Vad Mathiesen et al., 2011).

Carbon capture and storage (CCS) is an interesting alternative because it reduces CO₂ emissions while other technologies (even the emerging ones) can be properly developed. The most

common CCS technologies are absorption, adsorption, and separation by membranes and cryogenic separation (Pires et al., 2011). Among these possibilities, adsorption is of great interest due to its low energy consumption, low equipment costs, and easiness for application (Bahadori and Vuthaluru, 2009; Liu et al., 2011).

Activated carbons are porous materials with adsorptive properties due to their porosity, high surface area, and surface chemistry (Rodríguez-Reinoso, 1997). Activated carbons are widely used as adsorbents of gases (such as H₂S, SO_x, and NO_x), vapors, dyes, and heavy metals (Aliabadi et al., 2012; Bandosz, 2008; Duan et al., 2012; Furtado et al., 2013; Lemus et al., 2012; Ma et al., 2012; Zhang et al., 2013; Zhu et al., 2012). However, there is increasing scientific interest about the use of activated carbon to adsorb CO₂ (An et al., 2011; Aroua et al., 2008; Guo et al., 2006; Redondas et al., 2012; Somy et al., 2009).

Sewage sludge is a potential feedstock for producing activated carbons due to its carbonaceous content. Over the last years, a wealth of research has been conducted into the production of sewage-sludge-based adsorbents (SBAs) (Smith et al., 2009). Producing activated carbon from sewage sludge allows

using a waste, otherwise difficult to deal with, to obtain added-value adsorbents (Geethakarathi and Phanikumar, 2011; Monsalvo et al., 2012).

The objective of this study is to investigate the feasibility of the CO₂ capture using activated carbon obtained from thermally dried sewage sludge after chemical activation. Specifically, chemical activation with KOH and NaOH of previously pyrolyzed sewage sludge was carried out. As far as the authors know, there are no previous works in the literature dealing with CO₂ capture using activated carbon obtained from KOH and NaOH chemical activation of the pyrolyzed sewage sludge (PSS).

Experimental

Sewage sludge samples

The thermally dried sludge samples were received from an urban wastewater treatment plant located in Madrid, Spain. They were received as spherical aggregates, of approximately 1–4 mm in diameter. The physicochemical characteristics of the sewage sludge samples are shown in Table 1.

Pyrolysis and preliminary adsorption capacity determination tests

Different pyrolysis tests were carried out with small amounts of sample (around 150 mg) using a thermogravimetric analyzer (TGA) (model 2050 CE; TA Instruments, Spain). The aim of these tests was to determine the pyrolysis conditions that produce the PSS carbons with the highest CO₂ adsorption capacity. To make the overall process as simple as possible, the PSS carbons were produced from the sewage sludge as received, taking into account that extruded activated carbons (cylindrical shaped with diameters from 0.8 to 5 mm) are commonly used for gas-phase applications because of their low pressure drop, high mechanical strength, and low dust content. Three different

Table 2. Results of the adsorption capacity determination in pyrolysis tests

Pyrolysis Temperature (°C)	Heating Rate (°C/min)	Adsorption Capacity (%) ^a
400	10	0.5
	25	0.5
	50	0.7
600	10	0.8
	25	1.0
	50	0.9
800	10	1.0
	25	1.0
	50	0.9
900	10	0.9
	25	0.7
	50	0.9
1000	10	0.5
	25	0.8
	50	0.9

Notes: ^aRelative to the weight of the PSS sample.

heating rates (10, 25, and 50 °C/min) and five different final temperatures (400, 600, 800, 900, and 1000 °C) were tested under a flowing (100 mL/min) N₂ atmosphere (Table 2).

For each sample obtained after the pyrolysis tests, the CO₂ adsorption capacity was measured with the help of the TGA. The temperature was set at 25 °C under an inert atmosphere of N₂ (100 mL/min). At this temperature, the inert atmosphere was rapidly substituted by flowing (100 mL/min) CO₂. The sample weight increased while the CO₂ was being adsorbed and the adsorption capacity was determined by weighing when constant weight was reached.

Preparation of the sewage-sludge-based activated carbons

Once known, the pyrolysis conditions that produced the PSS samples with the highest adsorption capacities for CO₂ (i.e., heating rate of 25 °C/min to 600 °C and heating rate of 10 °C/min to 800 °C; Table 2), PSS carbons were produced at laboratory scale using a fixed-bed reactor of quartz heated by an electric furnace.

Two samples of sewage sludge of 100 g each were loaded into the reactor under an inert (N₂) atmosphere (150 mL/min). In both cases, the final pyrolysis temperatures of 600 and 800 °C were maintained over 30 min before cooling to ambient temperature. After pyrolysis, the PSS samples were subjected to different chemical activation processes adapted from Ros et al. (2006), using KOH and NaOH (Table 3).

Regarding chemical activation with KOH, 4 mL of a KOH (10 M) solution was added to 5 g of PSS. After 15 min of contact time, the mixture was filtrated and dried at 110 °C for 40 min. Later, each sample was loaded into the fixed-bed reactor under a flowing N₂ atmosphere (100 mL/min) and was heated at 5 °C/min to 700 °C. Once the maximum temperature was reached, a reaction time of 60 min was applied. After the heat treatment, samples

Table 1. Physicochemical characteristics of the sewage sludge (as received) and SBA_{T16} carbon

Parameter ^a	Sludge	SBA _{T16}	Analytical Method
Moisture (%)	6.3	—	UNE-EN 12880-2001
Organic matter (%)	55.8	28.9	UNE-EN 12879-2001
Ash (%)	44.2	71.1	UNE-EN 12879-2001
S _{BET} (m ² /g)	0.61	178.9	N ₂ adsorption isotherm
Carbon (%)	28.6	20.5	Elementary microanalyzer LECO CHNS-932
Nitrogen (%)	4.9	1.2	
Hydrogen (%)	4.5	1.1	
Sulfur (%)	1.1	0.1	

Notes: ^aDry-basis values, except moisture.

Table 3. Pyrolysis conditions, activation processes and adsorption capacities of the activated carbons

Test	Pyrolysis Conditions: Temperature (°C) / Heating Rate (°C/min)	Activating Agent	Heat treatment: Temperature (°C) / Heating Rate (°C/min) / Isotherm (min)	After treatment	Adsorption Capacity (%) ^a
1	600 / 25	—	—	—	1.0
2	800 / 10	—	—	—	1.0
3	600 / 25	KOH (10 M)	700 / 5 / 60	HCl (2 M) + H ₂ O	1.5
4	600 / 25	KOH (10 M)	700 / 5 / 60	HCl (5 M) + H ₂ O	2.1
5	800 / 10	KOH (10 M)	700 / 5 / 60	HCl (2 M) + H ₂ O	1.2
6	800 / 10	KOH (10 M)	700 / 5 / 60	HCl (5 M) + H ₂ O	1.8
7	800 / 10	Solid KOH	700 / 5 / 60	H ₂ O	1.7
8	800 / 10	Solid KOH	700 / 5 / 60	HCl (5 M) + H ₂ O	2.2
9	600 / 25	NaOH (10 M)	700 / 5 / 60	H ₂ O	1.0
10	800 / 10	NaOH (10 M)	700 / 5 / 60	H ₂ O	1.3
11	600 / 25	NaOH (10 M)	700 / 5 / 60	HCl (5 M)	0.6
12	800 / 10	NaOH (10 M)	700 / 5 / 60	HCl (5 M)	0.4
13	600 / 25	NaOH (10 M)	700 / 5 / 60	HCl (5 M) + H ₂ O	1.5
14	800 / 10	NaOH (10 M)	700 / 5 / 60	HCl (5 M) + H ₂ O	1.7
15	800 / 10	Solid NaOH	700 / 5 / 60	H ₂ O	2.2
16	800 / 10	Solid NaOH	700 / 5 / 60	HCl (5 M) + H ₂ O	3.8
17	Airpel 10	—	—	—	3.0

Notes: ^aRelative to the weight of the PSS sample (tests 1 and 2), to the weight of the SBA sample (tests 3–16), and to the weight of the Airpel 10 sample (test 17).

were mixed with either a HCl (2 M) or a HCl (5 M) solution over 15 min, and then washed with distilled water until absence of chloride ions in the washing water (pH = 6). Two tests were carried out with solid KOH. Specifically, 5 g of solid KOH were ground in a mill and directly mixed with the 5 g of PSS. After the heat treatment (N₂ atmosphere, 5 °C/min, 700 °C, 60-min isotherm), two different aftertreatments were applied: (i) the sample was thoroughly washed with distilled water until neutral pH in the washing water; and (ii) the sample was mixed with a HCl (5 M) solution over 15 min, then washed with distilled water until absence of chloride ions in the washing water.

As for chemical activation with NaOH, a similar methodology was followed but using 4 mL of a NaOH (10 M) solution. After the previously explained heat treatment, three different options were tested (Table 3): (i) the samples were washed only with distilled water until neutral pH; (ii) the samples were washed only with a HCl (5 M) solution over 15 min; and (iii) the samples were washed with a HCl (5 M) solution over 15 min and then with distilled water until absence of chloride ions in the washing water.

In the case of the activation with solid NaOH, the heat treatment was developed in a platinum capsule to prevent damage to the quartz reactor associated with the use of solid NaOH. In all cases, with both KOH and NaOH, the SBAs were dried at 110 °C overnight.

The adsorption capacity of the SBAs was again determined with the TGA over samples of 150 mg and the results were compared with those obtained with PSS carbons and with an extruded commercial activated carbon (Airpel 10; Desotec Activated Carbon, N.V.-S.A., Roeselare, Belgium) commonly used for gas adsorption (Joó et al., 2010; VOLTAIR, 2007) (Table 3).

Characterization of the adsorbents

Isothermal tests

The activated carbon with the highest adsorption capacity (test number 16, Table 3, hereafter SBA_{T16}) was investigated for its gaseous adsorption characteristics using CO₂. For this purpose, adsorption isotherms at 25 °C were carried out. A 70-mg sample of SBA_{T16} was loaded in the TGA under air atmosphere (100 mL/min) until weight stabilization. This air atmosphere was rapidly substituted by either flowing (100 mL/min) CO₂/air (20:80 v/v). Once constant weight was reached, the CO₂ concentration of the CO₂/air mixture was changed every 15 min (CO₂ concentration of 40%, 60%, 80%, and 100% v/v) and the weight change was calculated.

Adsorption results were modeled according to the Langmuir equation and the Freundlich equation.

Characterization of the physical structure

The PSS obtained after heating at 10 °C/min to 800 °C (test number 2, Table 3, hereafter PSS_{T2}) and the SBA_{T16} were characterized for their surface and pore characteristics using continuous volumetric nitrogen gas adsorption at 77 K in an ASAP2020 Surface area and porosimetry analyzer and mercury porosimetry in an AutoPore IV 9500 Mercury Porosimeter, both from Micromeritics (Bonsai Advanced Technologies, S.L., Spain). More precisely, the specific surface area was calculated using the Brunauer-Emmet-Teller (BET) equation (S_{BET} ; Brunauer et al., 1938), the micropore volume and the external surface area (S_{ext}) by *t*-method (Lowell and Shields, 1984), whereas the mesopore size distribution was estimated according to the Barrett-Joyner-Halenda (BJH) method (Barrett et al., 1951).

Results and Discussion

Pyrolyzed sewage sludge

The results of pyrolysis and preliminary adsorption capacity determination tests are summarized in Table 2. It can be seen that the two pyrolysis processes with the best results were obtained at a temperature of 600 °C and a heating rate of 25 °C/min as well as at a pyrolysis temperature of 800 °C and a heating rate of 10 °C/min. The higher adsorption capacities obtained at these temperatures are explained by the thermogravimetric results. Two main peaks were found in the weight-loss curves at around 300–400 and 600–700 °C, respectively. The devolatilization reactions associated with these peaks promote the development of the porosity in the carbonaceous material. Specifically, the adsorption capacity of the PSS obtained under these experimental conditions was 1.0% (related to the weight of the pyrolyzed sample) in both cases. Starting from these results, the products obtained in the pyrolysis processes at 600 and 800 °C were selected for superior tests, as explained in Experimental.

Sewage-sludge-based activated carbons

Table 3 shows the adsorption capacity of the different SBAs after chemical activation. It can be seen that the adsorption capacities obtained with both KOH and NaOH were quite similar in general terms.

Regarding chemical activation with KOH (10 M), the adsorption capacity of the SBAs varied between 1.2% and 2.1%, i.e., the adsorption capacity increased in the range of 20–110% in comparison with the values of the PSS samples (tests 1 and 2). Better results were found when solid KOH was used as activating agent, with improvements of the adsorption capacity between 70% and 120% with respect to PSS values.

As for chemical activation with NaOH (10 M), adsorption capacity values of up to 1.7% were found. Even though HCl has proven to increase the BET surface area of PSS carbons and SBAs (Ros et al., 2006), reductions in the adsorption capacity were detected when aftertreatment with HCl (5 M) was applied in tests 11 and 12. In this work, HCl is mainly used to neutralize excess NaOH or KOH after the activation process. When residual HCl is not washed (such as in tests 11 and 12), the acid keeps reacting during the subsequent drying step, inducing changes in the physical state of the material by the chemical degradation of the inorganic structure (Bagreev et al., 2001; Smith et al., 2009). As a consequence, a decrease in the adsorption capacity was observed.

As with KOH, better results were found when solid NaOH was used. In fact, the highest adsorption capacity value was detected for the test number 16, corresponding to 3.8% of the initial SBA weight. These results indicate that a better contact between the carbonaceous precursor and the hydroxide is produced when powdered hydroxides are used (Ros et al., 2006).

Comparing the results obtained with both activating agents, solid NaOH performed better than solid KOH. Where NaOH and KOH are used to activate different forms of carbonaceous materials, their relative effectiveness mainly depends on the hydroxide/precursor ratio, the type of precursor material, and the

material composition (Contreras et al., 2010; Maciá-Agulló et al., 2004, 2007; Raymundo-Piñero et al., 2005; Ros et al., 2006; Smith et al., 2009; Tseng, 2006; Zubizarreta et al., 2008, 2009). Special attention is directed to the contribution of the inorganic fraction (Lillo-Ródenas et al., 2008). According to these authors, KOH is more efficient in the development of porosity than NaOH when the material has some degree of crystallinity. However, NaOH performs better with disorganized precursors, such as those generated from sewage sludge.

Isothermal tests

Figure 1 shows the results obtained from the isothermal tests of the SBA_{T16}. The values of the isotherm constants and the correlation coefficient (R^2) of the data fittings to each of the models are shown in Table 4.

Regarding the Langmuir model, the adsorption capacity (Q) and the affinity value (b) were obtained from the equation presented in Figure 1a. The resulting adsorption capacity of the SBA_{T16} for CO₂ was close to 56 mg/g, which falls in the usually reported ranges in the literature for commercial and for

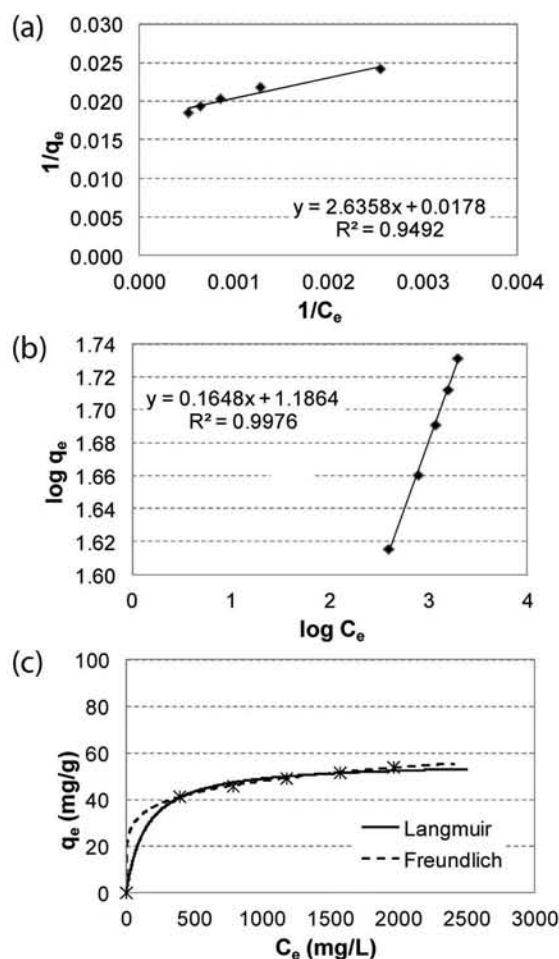


Figure 1. Results of the isothermal test. (a) Linearized Langmuir isotherm for CO₂ adsorption by SBA_{T16}. (b) Linearized Freundlich isotherm for CO₂ adsorption by SBA_{T16}. (c) Equilibrium adsorption isotherms of CO₂ onto SBA_{T16}.

Table 4. Langmuir and Freundlich isotherm parameters for CO₂ on SBA_{T16}

Langmuir Isotherm ^a				Freundlich Isotherm ^b		
R^2	Q (mg/g)	b	r	R^2	n	K_F
0.949	56.18	0.00675	0.0177	0.998	6.07	15.36

Notes: ^a Q and b , Langmuir constants related to maximum adsorption capacity and energy of adsorption, respectively. ^b n and K_F Freundlich constants indicating how favorable the adsorption is and the adsorption capacity of the sample, respectively.

palm-shell-based activated carbons (Aroua et al., 2008; Guo et al., 2006; Somy et al., 2009).

The essential characteristics of the Langmuir isotherm can be expressed in terms of the dimensionless constant separation factor or equilibrium parameter, r , defined as $[(1 + b) \times Q]^{-1}$. Adsorption is considered favorable when $r < 1$, irreversible when $r = 0$, lineal when $r = 1$, and unfavorable when $r > 1$ (Adebawale et al., 2006; Vadivelan and Kumar, 2005). Accordingly, the adsorption was found to be favorable ($r = 0.0177$).

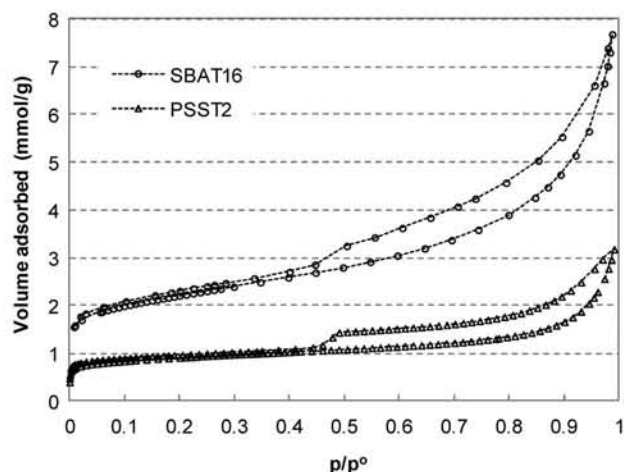
As for the Freundlich model, the constants n and K_F (indicating how favorable the adsorption is and the adsorption capacity of the sample, respectively) were calculated from the equation shown in Figure 1b. The obtained n value (6.07), which is greater than 1, suggests that CO₂ is favorably adsorbed by the SBA_{T16} (Rozada et al., 2003).

Both the correlation coefficients (Table 4) and the graphical representation (Figure 1c) showed higher agreement of the Freundlich isotherm with the experimental data.

Physical structure of the adsorbent

Figure 2 shows the nitrogen gas adsorption-desorption isotherms exhibited by both the PSS_{T2} and the SBA_{T16} samples. Regarding PSS_{T2} sample, most of the nitrogen adsorption occurs at high relative pressures, which denoted the presence of large mesopores. This type of isotherm is characteristic of mesoporous materials with a poorly developed micropore structure (Gregg and Sing, 1982). As for SBA_{T16}, the greater adsorption capacities observed at low relative pressures ($p/p^0 < 0.3$) reflected a more developed micropore structure. Additionally, the use of solid NaOH increased the formation of mesoporosity, as it can be deduced from the increase of the adsorption capacity detected at medium and high relative pressures and from the slope of the isotherm.

The BET surface area (S_{BET}), the external surface area (including mesopores and macropores area, S_{ext}), the micropores surface area (S_m), the total pore volume (V_t), the micropores

**Figure 2.** Nitrogen adsorption-desorption isotherms exhibited by the PSS_{T2} and the SBA_{T16} samples.

volume (V_m), and the average pore diameter ($4V/A$ by BET, D_p) of the samples are presented in Table 5.

The S_{BET} of both the PSS_{T2} and the SBA_{T16} was mainly composed of mesopores and macropores ($S_{ext} > S_{micro}$) and the average pore diameters (51.8 and 56.5 Å, respectively) informed about the mesoporous character of the samples. Even though the S_{BET} increased with the chemical activation, the values obtained were quite low, probably due to the fact that the sewage sludge was pyrolyzed as received. However, it is worth noticing that although the S_{BET} obtained for SBA_{T16} (179 m²/g) is well below than that of Airpel 10 (1020 m²/g), its adsorption capacity was higher (Table 3). The efficiency of the activated carbon depends on its accessible internal surface area (where physical adsorption takes place), and also on the presence of active sites where chemisorption may occur (Rodríguez-Reinoso, 1997). Therefore, the surface chemistry plays a very important role in the adsorptive properties of the material, an issue that would explain the better results obtained with the SBA_{T16}. The use of

Table 5. Physical characteristics of the PSS_{T2} and the SBA_{T16} from the N₂ adsorption isotherms

	S_{BET} (m ² /g)	S_{ext} (m ² /g)	% of S_{BET}	S_{micro} (m ² /g)	% of S_{BET}	V_t (mL/g)	V_{micro} (mL/g)	D_p (Å)
PSS _{T2}	74.2	45.9	61.77	28.4	38.23	0.096	0.0082	51.8
SBA _{T16}	178.9	132.3	73.96	46.6	26.04	0.253	0.0085	56.5

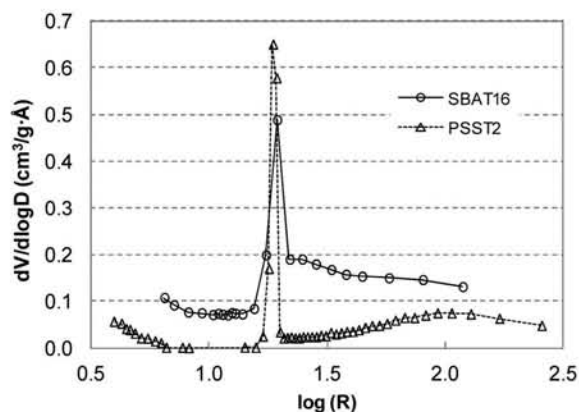


Figure 3. BJH mesopore size distribution of the PSS_{T2} and the SBA_{T16} samples. R expressed in Å.

NaOH as activating agent results in activated carbons with base sites where CO₂ is known to act as a Lewis acid (Siriwardane et al., 2003) enhancing the adsorption capacity of the sample.

The mesopore size distributions of the PSS_{T2} and the SBA_{T16} samples assessed according to BJH are shown in Figure 3.

It can be seen that the PSS_{T2} presented a narrow mesopore distribution with a peak occurring at approximate 37 Å ($\log R = 1.269$). The peak value of the distribution curve obtained for the SBA_{T16} was slightly shifted to 39 Å ($\log R = 1.287$) and the mesopore size distribution was widened as a result of the NaOH chemical activation, which is in agreement with the small increase of D_p found (Table 5).

Regarding macropores, Table 6 shows the main results of the mercury porosimetry.

It can be observed how the chemical activation with solid NaOH increased the porosity and the total volume of Hg adsorbed (V_{Hg}). Slight differences were found in the proportion of V_{Hg} corresponding to macropores and mesopore between the samples (V_{macro} and V_{meso} , respectively). Although most of V_{Hg} was related to macroporosity in both cases, there was an increase in the proportion of V_{meso} in SBA_{T16}. This result was in agreement with the decrease in the average pore diameter ($4V/A$, D_{pHg}).

The cumulative volume and the derivative pore size distribution curves obtained from mercury porosimetry as a function of the pore size for the PSS_{T2} and the SBA_{T16} are presented in Figure 4. The PSS_{T2} sample shown a bimodal pore size distribution with two peaks centered at 60 nm ($\log R = 1.477$) and 40 μm ($\log R = 4.301$) (Figure 4b). A similar pore size

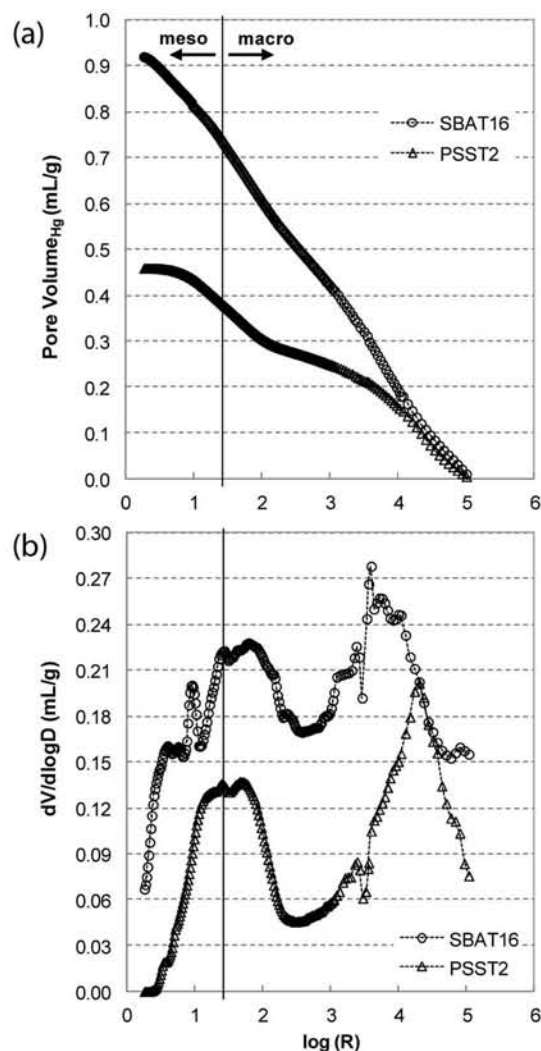


Figure 4. (a) Cumulative volume and (b) derivative pore size distribution curves as a function of the pore size for the PSS_{T2} and the SBA_{T16} samples obtained from mercury porosimetry. R expressed in nm.

distribution was found for SBA_{T16} but, in this case, the maximum peaks were found at 100 nm ($\log R = 1.698$) and 11 μm ($\log R = 3.740$). An additional peak was detected at 18 nm, probably as a result of the widening of micropores or small mesopores during chemical activation.

Scanning electron microscopy (SEM) was used to examine the surface characteristics of both the sewage sludge as received (Figure 5c) and the SBA_{T16} (Figure 5d). It can be observed that the sewage sludge surface (Figure 5c) was quite

Table 6. Results of the mercury porosimetry for the PSS_{T2} and the SBA_{T16}

	V_{Hg} (mL/g)	V_{macro} (mL/g)	% V_{Hg}	V_{meso} (mL/g)	V_{Hg}	D_p (nm)	Porosity(%) %
PSS _{T2}	0.46	0.38	83.7	0.07	16.3	99	49.5
SBA _{T16}	0.92	0.74	80.0	0.18	20.0	52	62.6

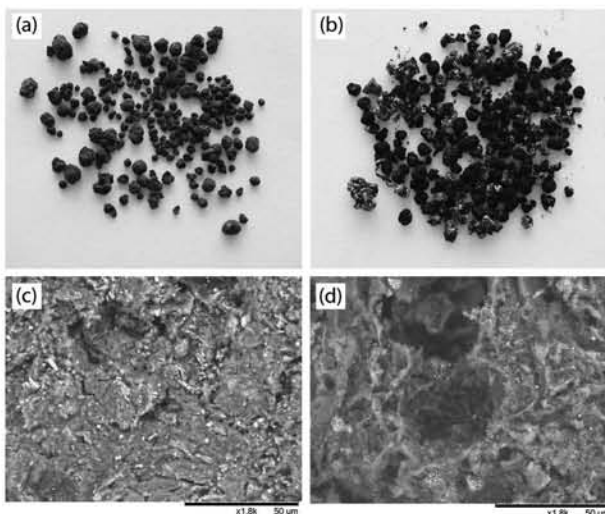


Figure 5. Photographs of (a) sewage sludge (as received) and (b) SBA_{T16}. SEM photographs in 1800 \times magnification of (c) sewage sludge (as received) and (d) SBA_{T16} carbon.

homogeneous and no relevant porosity was found. On the other hand, pores of different sizes can be observed in the SBA_{T16} surface (Figure 5d). The large macropores located in the middle of the picture were produced by the liberalization of volatiles during the pyrolysis stage. Inside the large macropores, the presence of smaller pores corresponding to small macropores and mesopores can be observed forming along the way followed by the adsorbate to reach the micropores (Rodríguez-Reinoso, 1997).

Conclusion

The work presented in this paper shows that sewage sludge can be used as precursor in the production of activated carbon for CO₂ adsorption, reducing greenhouse gas emissions and promoting the valorization of this waste.

To produce the activated carbons, chemical activations with KOH and NaOH of previously pyrolyzed sewage sludge (PSS) were carried out. Even though both chemicals clearly improved the adsorption capacity of the PSS samples, the highest adsorption capacities were found with NaOH, especially when it was used in solid form.

Adsorption isotherms were carried out over the activated carbon with the highest adsorption capacity (SBA_{T16}). Adsorption results were modeled according to the Langmuir and Freundlich models, with resulting CO₂ adsorption capacities close to 56 mg/g, which fall in the ranges usually reported in the literature for commercial and for palm-shell-based activated carbons.

The SBA_{T16} presented mesoporous character. The BET surface area (S_{BET}) was mainly contributed by mesopores and macropores. Although S_{BET} was low (179 m²/g) in comparison with that of a commercial activated carbon (Airpel 10; 1020 m²/g) its adsorption capacity was higher because the use of NaOH increased CO₂ chemisorption.

The work presented here shows that sewage sludge is a promising and interesting feedstock for producing activated carbons suitable for CO₂ adsorption. However, further research is needed on the improvement of their adsorption capacity through a better control of the pyrolysis and the chemical activation processes.

Acknowledgment

This work has been partially funded by a grant from the REPSOL Foundation.

References

- Adams, T.A., II, and P.I. Barton. 2011. Combining coal gasification and natural gas reforming for efficient polygeneration. *Fuel Process. Technol.* 92:639–655. doi:10.1016/j.fuproc.2010.11.023
- Adams, T.A., II, and P.I. Barton. 2010. High-efficiency power production from natural gas with carbon capture. *J. Power Sources* 195:1971–1983. doi:10.1016/j.jpowsour.2009.10.046
- Adebawale, K.O., I.E. Unuabonah, and B.I. Olu-Owolabi. 2006. The effect of some operating variables on the adsorption of lead and cadmium ions on kaolinite clay. *J. Hazard. Mater.* 134:130–139. doi:10.1016/j.jhazmat.2005.10.056
- Aliabadi, M., I. Khazaei, H. Fakhraee, and M.T.H. Mousavian. 2012. Hexavalent chromium removal from aqueous solutions by using low-cost biological wastes: Equilibrium and kinetic studies. *Int. J. Environ. Sci. Technol.* 9:319–326. doi:10.1007/s13762-012-0045-7
- An, H., B. Feng, and S. Su. 2011. CO₂ capture by electrothermal swing adsorption with activated carbon fibre materials. *Int. J. Green. Gas Control* 5:16–25. doi:10.1016/j.ijggc.2010.03.007
- Aroua, M.K., W.M.A.W. Daud, C.Y. Yin, and D. Adinata. 2008. Adsorption capacities of carbon dioxide, oxygen, nitrogen and methane on carbon molecular basket derived from polyethyleneimine impregnation on microporous palm shell activated carbon. *Sep. Purif. Technol.* 62:609–613. doi:10.1016/j.seppur.2008.03.003
- Bagreev, A., T.J. Bandosz, and D.C. Locke. 2001. Pore structure and surface chemistry of adsorbents obtained by pyrolysis of sewage sludge-derived fertilizer. *Carbon* 39:1971–1979. doi:10.1016/S0008-6223(01)00026-4
- Bahadori, A., and H.B. Vuthaluru. 2009. New method accurately predicts carbon dioxide equilibrium adsorption isotherms. *Int. J. Green. Gas Control* 3:768–772. doi:10.1016/j.ijggc.2009.07.003
- Bandosz, T.J. 2008. Removal of inorganic gases and VOCs on activated carbons. In *Adsorption by Carbons*, ed. E.J. Bottani and J.M.D. Tascón, 533–564. Oxford, UK: Elsevier Science.
- Barrett, E.P., L.G. Joyner, and P.P. Halenda. 1951. The determination of pore volumes and area distributions in porous substances. *J. Am. Chem. Soc.* 73:373–380. doi:10.1021/ja01145a126
- Beér, J.M., 2007. High efficiency electric power generation: The environmental role. *Prog. Energ. Combust.* 33:107–134. doi:10.1016/j.pecs.2006.08.002
- Brunauer, S., P.H. Emmet, and F. Teller. 1938. Surface area measurements of activated carbons, silica gel and other adsorbents. *J. Am. Chem. Soc.* 60:309–319. doi:10.1021/ja01269a023
- Contreras, M. S., C.A. Páez, L. Zubizarreta, A. Léonard, S. Blacher, C.G. Olivera-Fuentes, and A. Arenillas. 2010. A comparison of physical activation of carbon xerogels with carbon dioxide with chemical activation using hydroxides. *Carbon* 48:3157–3168. doi:10.1016/j.carbon.2010.04.054
- Duan, X.-H., C. Srinivasa Kannan, W.-W. Qu, X. Wang, J.-H. Peng, L.-B. Zhang, and H.-Y. Xia. 2012. Thermal regeneration of spent coal-based activated carbon using carbon dioxide: Process optimisation, Methylene Blue decolorisation isotherms and kinetics. *Color. Technol.* 128:464–472. doi:10.1111/j.1478-4408.2012.00401.x
- Furtado, A.M.B., Y. Wang, and M.D. Levan. 2013. Carbon silica composites for sulfur dioxide and ammonia adsorption. *Micropor. Mesopor. Mater.* 165:48–54. doi:10.1016/j.micromeso.2012.07.032

- Geethakarthis, A., and B.R. Phanikumar. 2011. Adsorption of reactive dyes from aqueous solutions by tannery sludge developed activated carbon: Kinetic and equilibrium studies. *Int. J. Environ. Sci. Technol.* 8:561–570.
- Gregg, S.J., and K.S.W. Sing. 1982. *Adsorption, Surface Area and Porosity*. London: Academic Press.
- Gross, R., M. Leach, and A. Bauen. 2003. Progress in renewable energy. *Environ. Int.* 29:105–122. doi:10.1016/S0160-4120(02)00130-7
- Guo, B., L. Chang, and K. Xie. 2006. Adsorption of carbon dioxide on activated carbon. *J. Nat. Gas Chem.* 15:223–229. doi:10.1016/S1003-9953(06)60030-3
- Intergovernmental Panel on Climate Change. 2007. *Climate Change 2007: Synthesis Report*. Contribution of Working Groups I, II and III to the Fourth Assessment Report of the Intergovernmental Panel on Climate Change (Core Writing Team, R.K. Pachauri and A. Reisinger, eds.). Geneva: Intergovernmental Panel on Climate Change.
- Joó, É., H. Van Langenhove, M. Šimpraga, K. Steppe, C. Amelynck, N. Schoon, J.F. Müller, and J. Dewulf. 2010. Variation in biogenic volatile organic compound emission pattern of *Fagus sylvatica* L. due to aphid infection. *Atmos. Environ.* 44:227–234. doi:10.1016/j.atmosenv.2009.10.007
- Lanzi, E., E. Verdolini, and I. Hašič. 2011. Efficiency-improving fossil fuel technologies for electricity generation: Data selection and trends. *Energy Policy* 39:7000–7014.
- Lemus, J., M. Martín-Martínez, J. Palomar, L. Gomez-Sainero, M.A. Gilarranz, and J.J. Rodríguez. 2012. Removal of chlorinated organic volatile compounds by gas phase adsorption with activated carbon. *Chem. Eng. J.* 211–212:246–254. doi:10.1016/j.cej.2012.09.021
- Lillo-Ródenas, M.A., A. Ros, E. Fuente, M.A. Montes-Morán, M.J. Martín, and A. Linares-Solano. 2008. Further insights into the activation process of sewage sludge-based precursors by alkaline hydroxides. *Chem. Eng. J.* 142:168–174. doi:10.1016/j.cej.2007.11.021
- Liu, S.H., Y.C. Lin, Y.C. Chien, and H.R. Hyu. 2011. Adsorption of CO₂ from flue gas streams by a highly efficient and stable aminosilica adsorbent. *J. Air Waste Manage. Assoc.* 61:226–233. doi:10.3155/1047-3289.61.2.226
- Lowell, S., and J.E. Shields. 1984. *Powder Surface Area and Porosity*, 2nd ed. New York: John Wiley.
- Ma, S.C., J.J. Yao, L. Gao, X.Y. Ma, and Y. Zhao. 2012. Experimental study on removals of SO₂ and NO_x using adsorption of activated carbon/microwave desorption. *J. Air Waste Manage. Assoc.* 62:1012–1021. doi:10.1080/10962247.2012.695320
- Maciá-Agulló, J.A., B.C. Moore, D. Cazorla-Amorós, and A. Linares-Solano. 2004. Activation of coal tar pitch carbon fibres: Physical activation vs. chemical activation. *Carbon* 42:1367–1370. doi:10.1016/j.carbon.2004.01.013
- Maciá-Agulló, J.A., B.C. Moore, D. Cazorla-Amorós, and A. Linares-Solano. 2007. Influence of carbon fibres crystallinities on their chemical activation by KOH and NaOH. *Micropor. Mesopor. Mater.* 101:397–405. doi:10.1016/j.micromeso.2006.12.002
- Monsalvo, V.M., A.F. Mohedano, and J.J. Rodríguez. 2012. Adsorption of 4-chlorophenol by inexpensive sewage sludge-based adsorbents. *Chem. Eng. Res. Des.* 90:1807–1814. doi:10.1016/j.cherd.2012.03.018
- Muis, Z.A., H. Hashim, Z.A. Manan, F.M. Taha, and P.L. Douglas. 2010. Optimal planning of renewable energy-integrated electricity generation schemes with CO₂ reduction target. *Renew. Energy* 35:2562–2570. doi:10.1016/j.renene.2010.03.032
- Peng, Y., B. Zhao, and L. Li. 2012. Advance in post-combustion CO₂ capture with alkaline solution: A brief review. *Energy Procedia* 14:1515–1522. doi:10.1016/j.egypro.2011.12.1126
- Pires, J.C.M., F.G. Martins, M.C.M. Alvim-Ferraz, and M. Simões. 2011. Recent developments on carbon capture and storage: An overview. *Chem. Eng. Res. Des.* 89:1446–1460. doi:10.1016/j.cherd.2011.01.028
- Polyzakis, A.L., C. Koroneos, and G. Xydis. 2008. Optimum gas turbine cycle for combined cycle power plant. *Energy Convers. Manage.* 49:551–563. doi:10.1016/j.enconman.2007.08.002
- Raymundo-Piñero, E., P. Azañ, T. Cacciaguerra, D. Cazorla-Amorós, A. Linares-Solano, and F. Béguin. 2005. KOH and NaOH activation mechanisms of multiwalled carbon nanotubes with different structural organisation. *Carbon* 43:786–795. doi:10.1016/j.carbon.2004.11.005
- Redondas, V., X. Gómez, S. García, C. Pevida, F. Rubiera, A. Morán, and J.J. Pis. 2012. Hydrogen production from food wastes and gas post-treatment by CO₂ adsorption. *Waste Manage.* 32:60–66. doi:10.1016/j.wasman.2011.09.003
- Rodríguez-Reinoso, F. 1997. Activated carbon: Structure, characterization, preparation and applications. In *Introduction to Carbon Technologies*, ed. H. Marsh, E.A. Heintz, and F. Rodríguez-Reinoso, 35–101. Secretariado de Publicaciones, Universidad de Alicante.
- Ros, A., M.A. Lillo-Ródenas, E. Fuente, M.A. Montes-Morán, M.J. Martín, and A. Linares-Solano. 2006. High surface area materials prepared from sewage sludge-based precursors. *Chemosphere* 65:132–140. doi:10.1016/j.chemosphere.2006.02.017
- Rozada, F., L.F. Calvo, A.I. García, J. Martín-Villacorta, and M. Otero. 2003. Dye adsorption by sewage sludge-based activated carbons in batch and fixed-bed systems. *Bioresour. Technol.* 87:221–230. doi:10.1016/S0960-8524(02)00243-2
- Siriwardane, R.V., M.S. Shen, and E.P. Fisher. 2003. Adsorption of CO₂, N₂, and O₂ on natural zeolites. *Energy Fuel* 17:571–576. doi:10.1021/ef0201351
- Smith, K.M., G.D. Fowler, S. Pullket, and N.J.D. Graham. 2009. Sewage sludge-based adsorbents: A review of their production, properties and use in water treatment applications. *Water Res.* 43:2569–2594. doi:10.1016/j.watres.2009.02.038
- Somy, A., M.R. Mehria, H.D. Amrei, A. Ghanizadeh, and M. Safari. 2009. Adsorption of carbon dioxide using impregnated activated carbon promoted by zinc. *Int. J. Green. Gas Control* 3:249–254. doi:10.1016/j.ijggc.2008.10.003
- Tseng, R.L. 2006. Mesopore control of high surface area NaOH-activated carbon. *J. Colloid Interf. Sci.* 303:494–502. doi:10.1016/j.jcis.2006.08.024
- Vadivelan, V., and K.V. Kumar. 2005. Equilibrium, kinetics, mechanism, and process design for the sorption of methylene blue onto rice husk. *J. Colloid Interf. Sci.* 286:90–100. doi:10.1016/j.jcis.2005.01.007
- Vad Mathiesen, B., H. Lund, and K. Karlsson. 2011. 100% Renewable energy systems, climate mitigation and economic growth. *Appl. Energy* 88:488–501. doi:10.1016/j.apenergy.2010.03.001
- VOLTAIR, 2007. *A Novel Hybrid Regenerating Filter for Improving Air Quality by Safely Destroying Biologically Active Airborne Particulates in Agri-Food Production Operations*. Co-operative Research (CRAFT—6th Framework Programme). Final activity report.
- Zecca, A., and L. Chiari. 2010. Fossil-fuel constraints on global warming. *Energy Policy* 38:1–3. doi:10.1016/j.enpol.2009.06.068
- Zhang, Z., I.M. O'Hara, G.A. Kent, and W.O.S. Doherty. 2013. Comparative study on adsorption of two cationic dyes by milled sugarcane bagasse. *Ind. Crop. Prod.* 42:41–49. doi:10.1016/j.indcrop.2012.05.008
- Zhu, Y., H. Zhang, H. Zeng, M. Liang, and R. Lu. 2012. Adsorption of chromium (VI) from aqueous solution by the iron (III)-impregnated sorbent prepared from sugarcane bagasse. *Int. J. Environ. Sci. Technol.* 9:463–472. doi:10.1007/s13762-012-0043-9
- Zubizarreta, L., A. Arenillas, J.P. Pirard, J.J. Pis, and N. Job. 2008. Tailoring the textural properties of activated carbon xerogels by chemical activation with KOH. *Micropor. Mesopor. Mater.* 115:480–90. doi:10.1016/j.micromeso.2008.02.023
- Zubizarreta, L., A. Arenillas, J.J. Pis, J.P. Pirard, and N. Job. 2009. Studying chemical activation in carbon xerogels. *J. Mater. Sci.* 44:6583–6590. doi:10.1007/s10853-009-3918-5

About the Authors

Juan Manuel de Andrés is a Ph.D. researcher, **Adolfo Narros** and **María del Mar de la Fuente** are lecturers, and **María Encarnación Rodríguez** is a professor at the Department of Chemical and Environmental Engineering, Technical University of Madrid (UPM).

Luis Orjales is a chemical engineering graduate at the Technical University of Madrid (UPM).